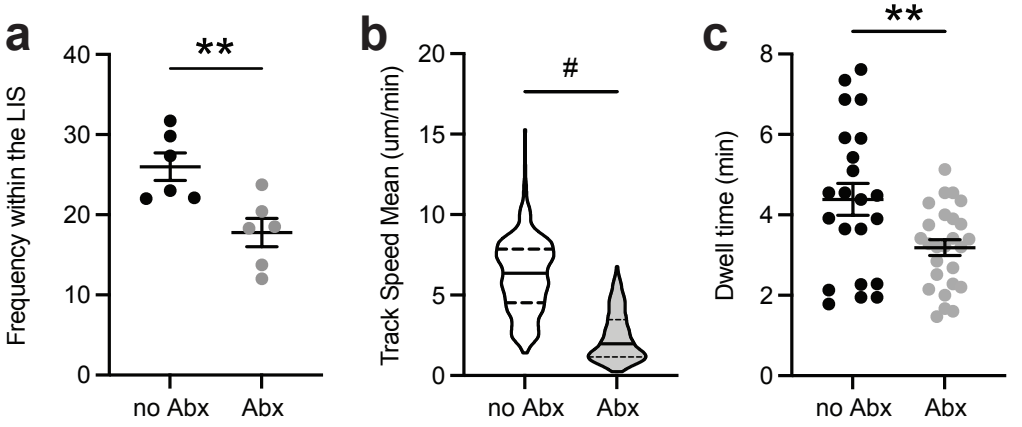

Figure S1. Commensal bacteria promote γδ IEL surveillance behavior. a Frequency of γδ IELs in the lateral intercellular space (LIS), **b** track speed mean and **c** dwell time in LIS were analyzed from intravital imaging of jejunal mucosa of untreated or antibiotic (Abx)-treated TcrdEGFP mice. Data are from two independent experiments, n=6. Each data point represents an individual mouse **a** or track **b,c.** Data represent mean (±SEM). Statistical analysis: unpaired t-test. **P<0.01, # P<0.0001.

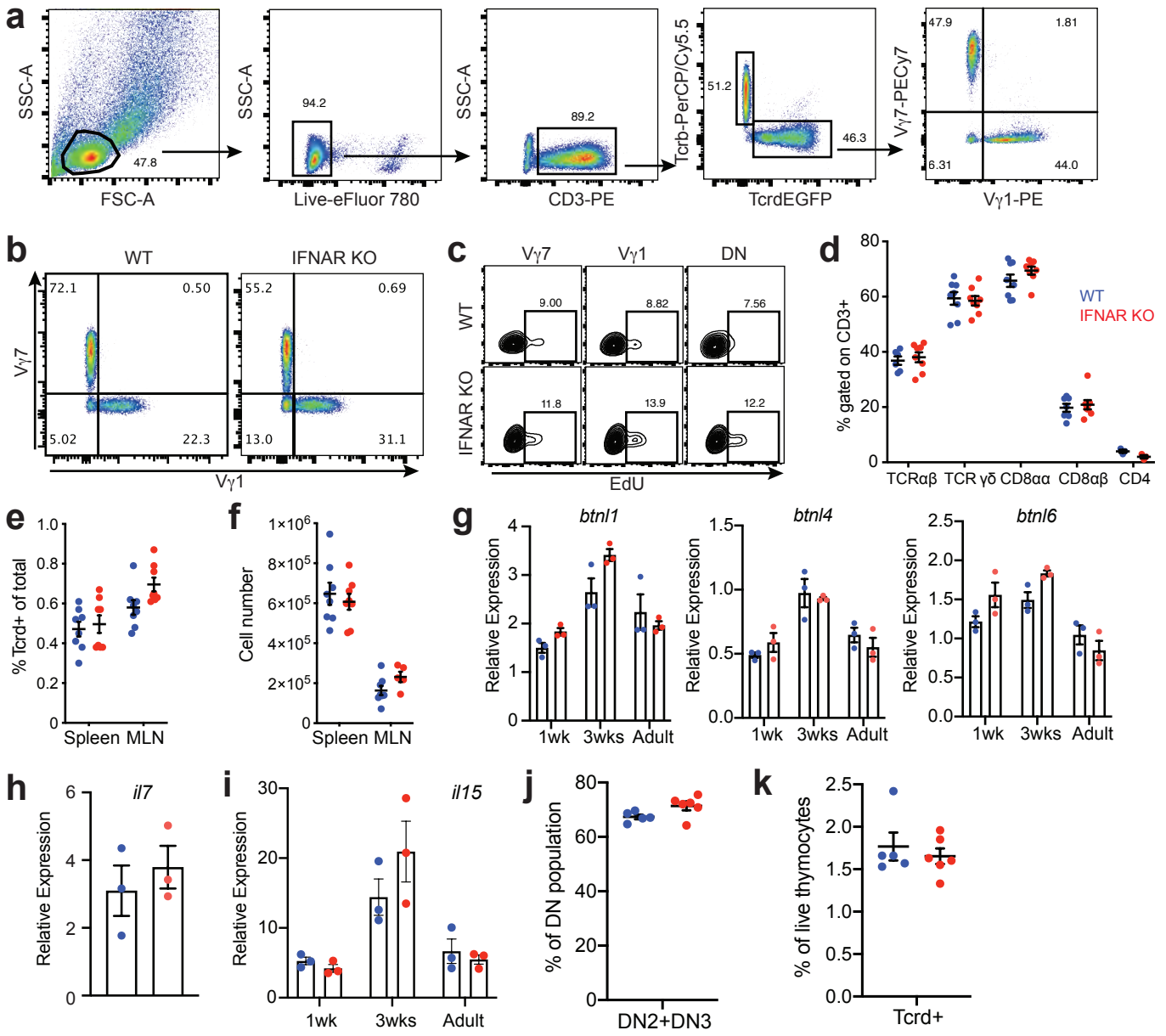

Figure S2. Loss of IFNAR does not alter peripheral γδ T cells, thymic γδ development or gut-intrinsic factors involved in IEL composition. a Gating strategy for the identification of IEL subsets. **b** Representative plot of Vγ1$^+$ and Vγ7$^+$ IELs and **c** EdU$^+$ populations within Vγ7$^+$, Vγ1$^+$, and double negative (DN) IEL populations in WT-S and IFNAR KO-S mice. **d** Phenotyping of small intestinal IEL compartment, n=6-8. **e** Frequency of Tcrd$^+$ and **f** total number of γδ T cells in spleen and mesenteric lymph nodes (MLN), n=6-8. **g** Relative expression of butyrophilin-like (btnl) 1,4,6, **h** interleukin (IL)-7 or **i** IL-15 in full thickness jejunum from WT and IFNAR KO mice as measured by quantitative real-time PCR, n=3. Frequency of **j** CD25$^+$ DN2 and DN3 T cell precursors and **k** Tcrd$^+$ cells gated on live thymocytes in E18.5 WT-S and IFNAR KO-S mice. Data represent the mean (±SEM) from 2-3 independent experiments. Each data point represents an individual mouse. Statistical analysis: unpaired t-test.

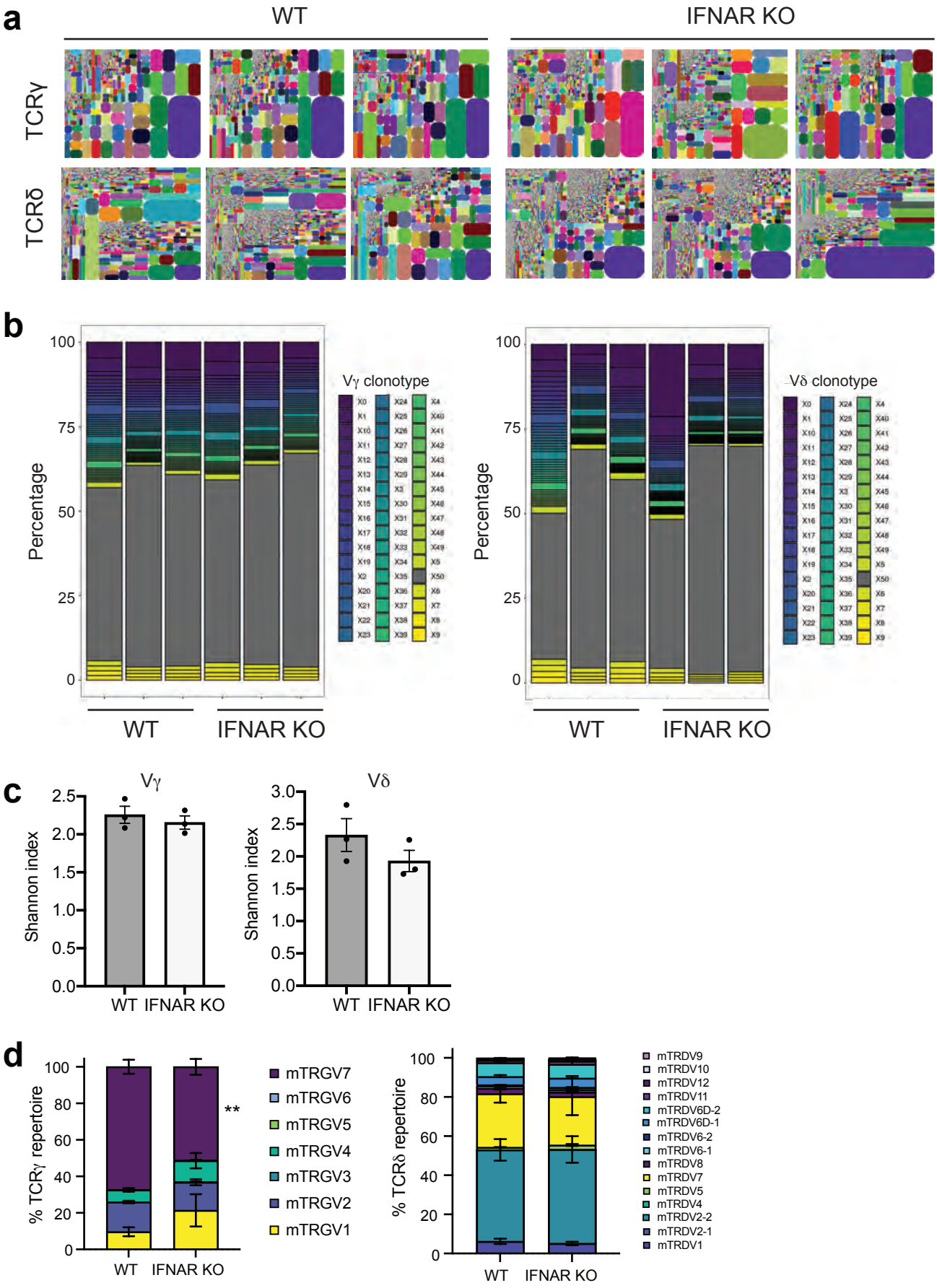

Figure S3. IFNAR-deficient γδ IELs exhibit comparable TCRγδ repertoires.a Representative tree maps of CDR3 clonotype usage in γδ IELs sorted from WT-S and IFNAR KO-S mice, n=3. **b** Frequency of CDR3 length usage for Vγ or Vδ subsets. **c** Shannon index of TCR diversity. **d** Percentage of TCRγ and TCRδ chain usage within the repertoire. Data represent mean (±SEM). Statistical analysis: **c:** unpaired t-test; **d:** two-way ANOVA with Sidak's post hoc test.

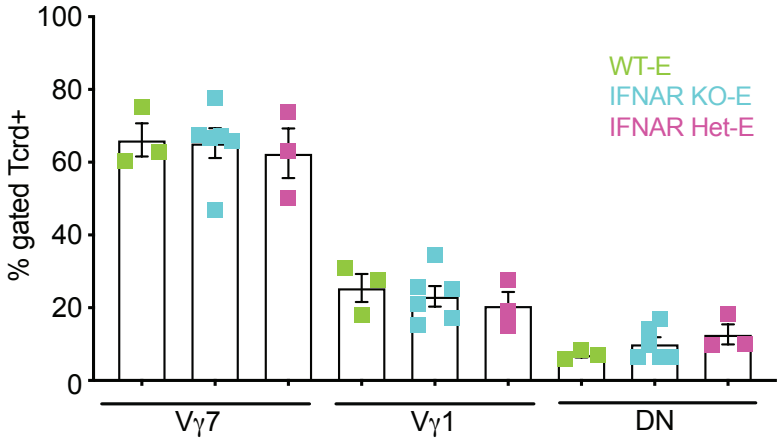

Figure S4. Vγ subsets are unchanged in IELs isolated from IFNAR KO-E mice. Frequency of Vγ subsets in IEL compartment from IFNAR KO-E mice. Data represent the mean (±SEM) from two independent experiments. Each data point represents an individual mouse. Statistical analysis: unpaired t-test compared to separately housed WT-S values.

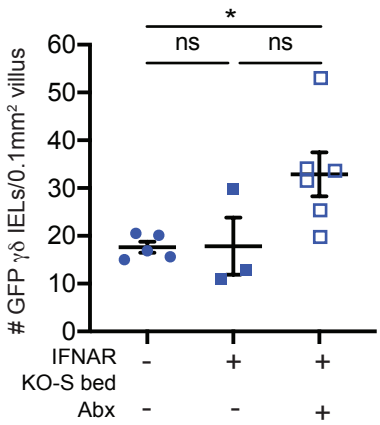

Figure S5. Microbiota from IFNAR KO-S mice fail to colonize WT-S mice. Morphometric analysis of the number of GFP⁺ γδ T cells in untreated WT-S, WT-S adults following IFNAR KO-S bedding transfer in the presence or absence of antibiotic (Abx) pre-treatment. n=3-6. Data represent mean (±SEM). Each data point represents an individual mouse. Statistical analysis: one-way ANOVA with Tukey's post hoc test *P<0.05

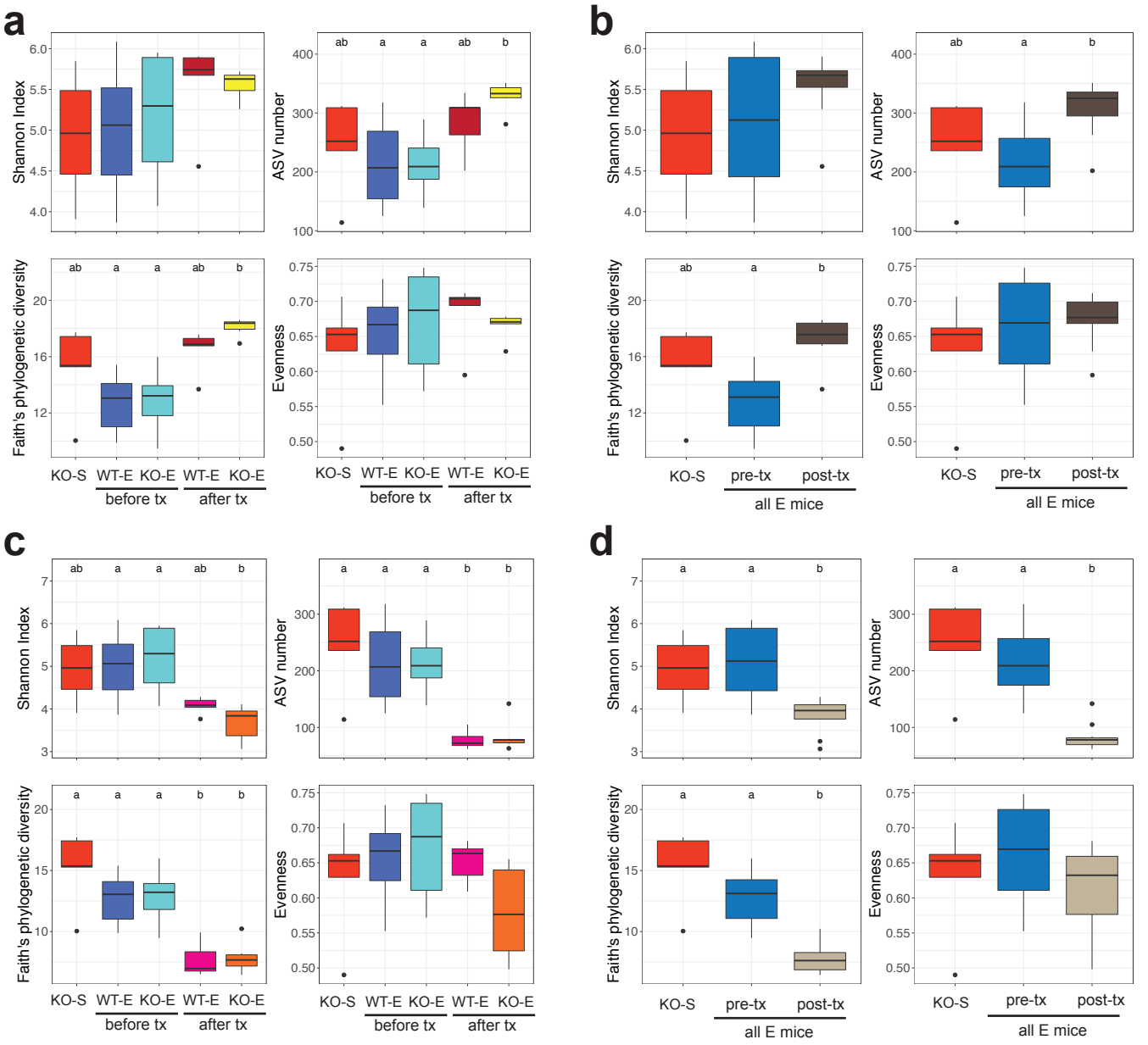

Figure S6. Microbial diversity is altered following horizontal transfer of IFNAR KO-S microbiota. Difference in alpha diversity of the gut microbiota between the different treatment groups. **a** Between IFNAR KO-S (donor), WT-E (pre-transfer), IFNAR KO-E (pre-transfer), WT-E (post-transfer) and IFNAR KO-E (post-transfer) **b** Between IFNAR KO-S, all E mice (pre-transfer) and all E mice (post-transfer) groups **c** Between IFNAR KO-S, WT-E (pre-transfer), IFNAR KO-E (pre-transfer), WT-E offspring (post-transfer) and IFNAR KO-E offspring (post-transfer) **d** Between IFNAR KO-S, all E mice (pre-transfer) and all E offspring mice (post-transfer) groups. Shannon Index, ASV numbers, Faith's phylogenetic diversity and Evenness were used as the indices to reflect the alpha diversity. Statistical analysis: Kruskal-Wallis test followed by Dunn's post hoc. Compact letters were used to show the significant differences between the groups. $P<0.05$ considered as significant.

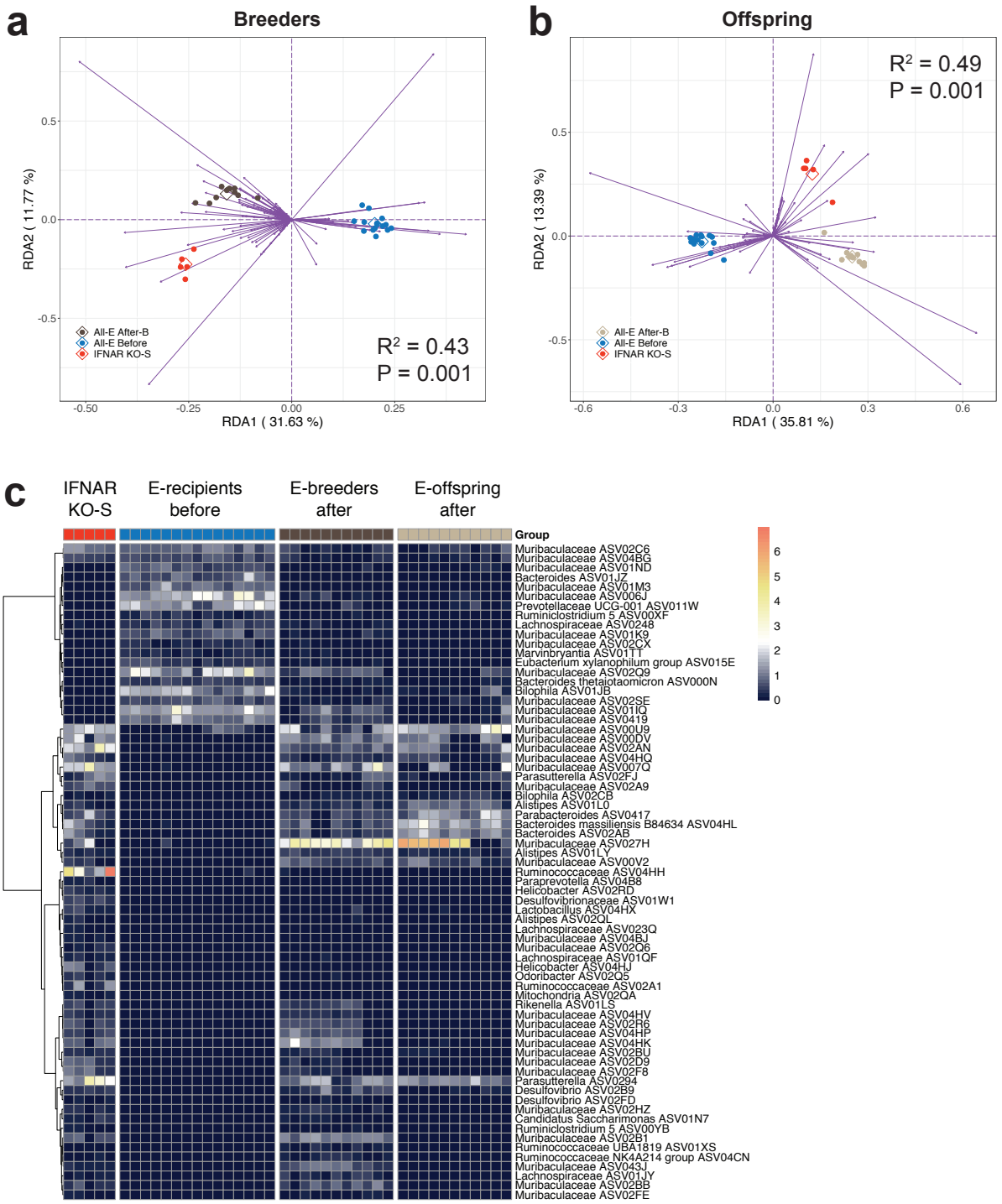

Figure S7. Differential microbial members are identified by redundancy analysis. Tri-plot of redundancy analysis (RDA) of the microbiota in the datasets containing **a** IFNAR KO-S, all E (pre-transfer) and all E breeders (post-transfer) groups and **b** IFNAR KO-S, all E (pre-transfer) and all E offspring (post-transfer) groups. Group information was used as the environmental variable. Hellinger transformed abundance of the (amplicon sequence variants) ASVs were used in the RDA analysis. Samples are indicated by dots. ASVs with more than 50% of the variability in their abundance explained by RDA1 and RDA2 are indicated by purple arrows. **c** The abundance heatmap of the 69 ASVs identified in both **a** and **b**. The heatmap shows the square-root transformed relative abundance of the ASVs. ASVs were clustered by ward linkage based on Spearman's correlation coefficient.

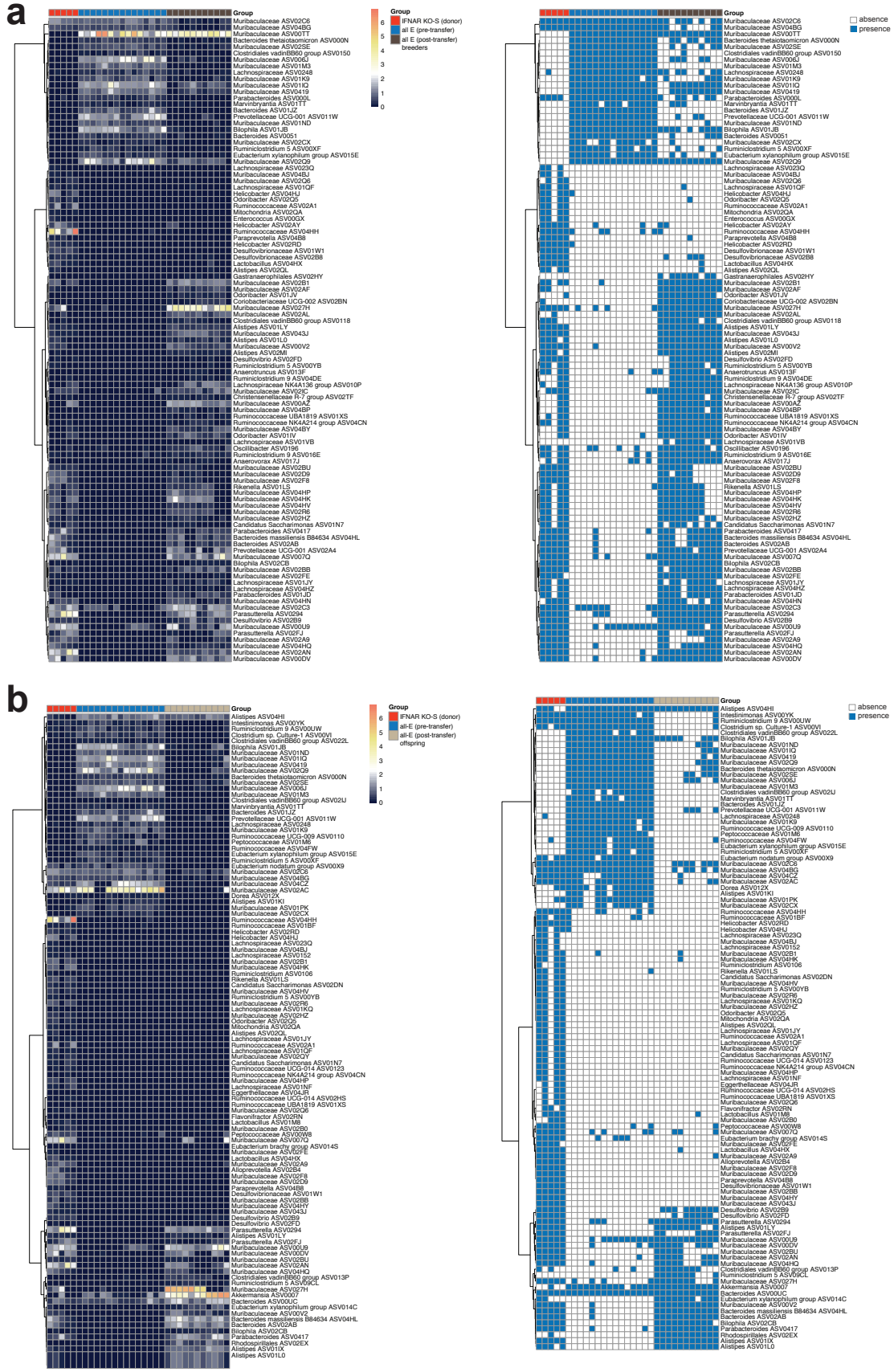

Figure S8. Heatmaps showing the detail abundance and occurrence information of the ASVs as identified by redundancy analysis.a The abundance heatmap shows the square-root transformed relative abundance **of the** 101 ASVs identified in Fig. S6**a. b** The abundance heatmap shows the square-root transformed relative abundance of the 108 ASVs identified in Fig. S6**b.** ASVs were clustered by ward linkage based on Spearman's correlation coefficient. Blue and white colors in occurrence heatmap show the presence and absence of the ASVs respectively.

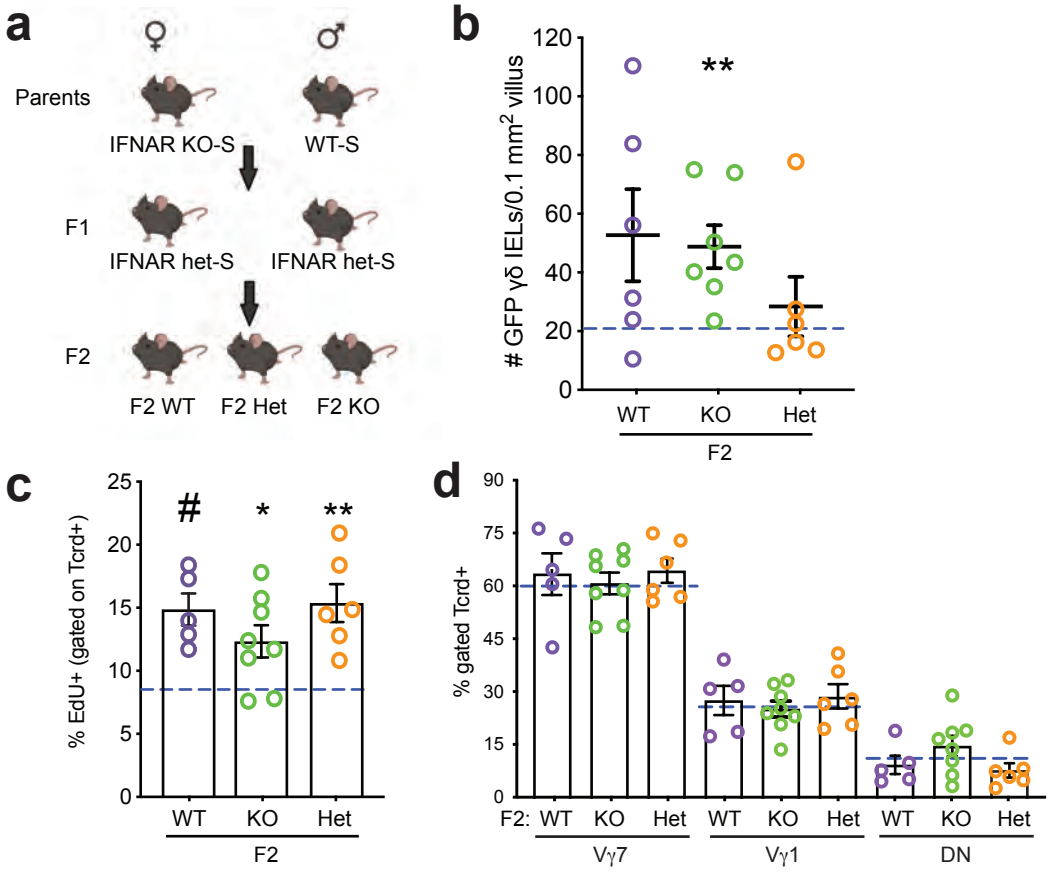

Figure S9. The genotype of the dam does not affect vertical transmission of the γδ IEL hyperproliferative phenotype. **a** Breeding strategy used to generate F2 WT and IFNAR KO littermates. **b** Morphometric analysis of GFP$^+$ γδ T cells in the jejunum of adult F2 littermates. **c** Percentage of EdU$^+$ γδ IELs and **d** proportion of Vγ IEL subsets in adult F2 littermates. Dashed lines indicate separately housed WT-S values. n=5-8 mice. Data represent mean (±SEM) from two independent experiments. Each data point represents an individual mouse. Statistical analysis: **b,c**: unpaired t-test; **d**: one-way ANOVA with Dunnett's post hoc test; All comparisons were made to separately housed WT-E values. *P<0.05, **P<0.01, #P<0.0001.

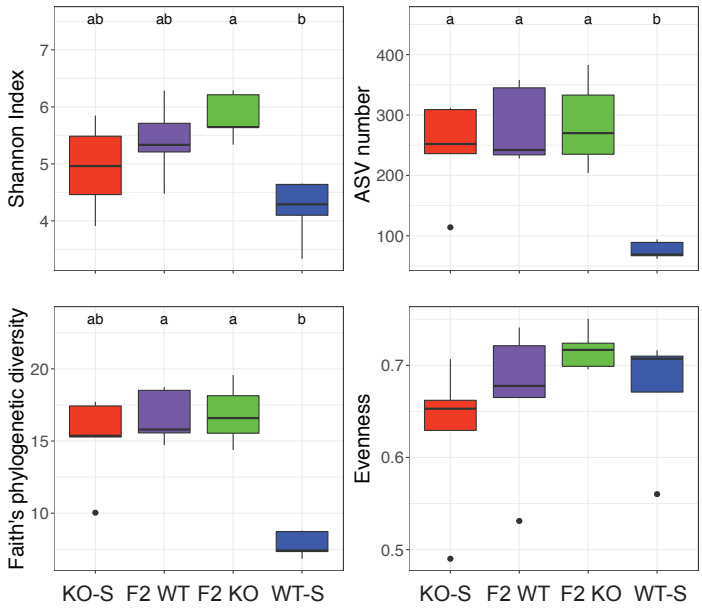

Figure S10. Microbial diversity is altered following vertical transfer of IFNAR KO-S microbiota. Difference in alpha diversity of the gut microbiota between the different treatment groups in the vertical transmission dataset. Shannon Index, ASV numbers, Faith's phylogenetic diversity and Evenness were used as the indices to reflect the alpha diversity. Statistical analysis: Kruskal-Wallis test followed by Dunn's post doc. Compact letters were used to show significance. $P<0.05$

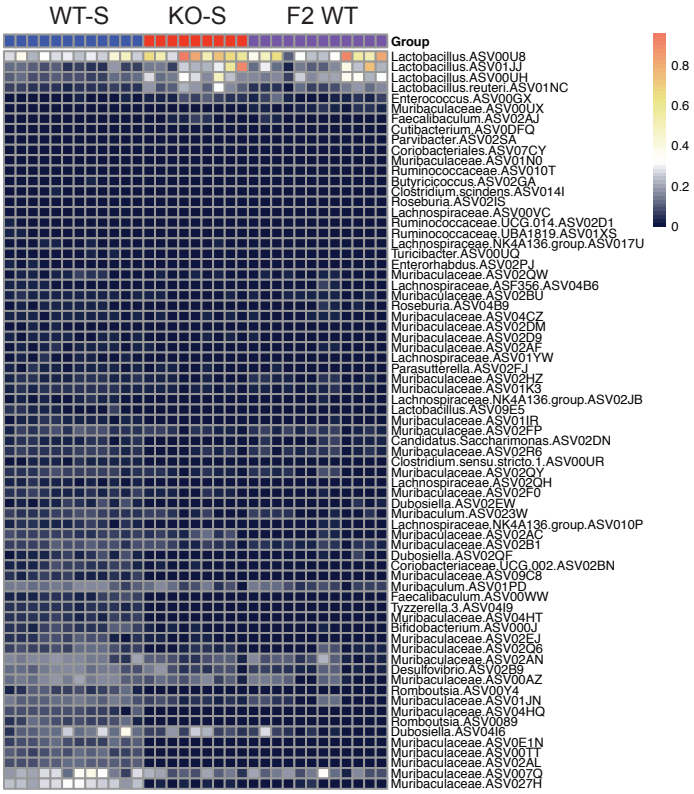

Figure S11. Seven ASVs are enriched in the small intestine of mice with the γδ IEL hyperproliferative phenotype. MaAsLin2 was applied to explore the differential ASVs in the small intestinal samples (duodenum, jejunum and ileum) between those mice with (IFNAR KO-S and F2 WT) and without the γδ IEL hyperproliferative phenotype (WT-S). The heatmap shows the arcsine square root transformed abundance of the significantly different ASVs. BH-adjusted p values < 0.05 considered as significant. The top seven ASVs were enriched in phenotypic mice.

Table S1. PERMANOVA test based on Bray Curtis distance showed significant differences in microbial composition between phenotypic (IFNAR KO-S and F2 WT) and non-phenotypic (WT-S) mice in each of the small intestinal segment

Pairs	R^2	P value	Segment
WT-S vs IFNAR KO-S	0.73330855	0.02857143	duodenum
WT-S vs F2 WT	0.242029018	0.0277	duodenum
IFNAR KO-S vs F2 WT	0.446258252	0.08571429	duodenum
WT-S vs IFNAR KO-S	0.546589514	0.02857143	jejunum
WT-S vs F2 WT	0.303981947	0.0277	jejunum
IFNAR KO-S vs F2 WT	0.221013092	0.28571429	jejunum
WT-S vs IFNAR KO-S	0.405456062	0.02857143	ileum
WT-S vs F2 WT	0.477266021	0.0277	ileum
IFNAR KO-S vs F2 WT	0.133409151	0.48571429	ileum

Table S2. PERMANOVA test based on Bray Curtis distance showed no difference in the overall microbial composition between different small intestinal segments within each group

Pairs	R^2	P value	Group
Duodenum vs Jejunum	0.04979145	0.8853	WT-S
Duodenum vs Ileum	0.08233548	0.6908	WT-S
Jejunum vs Ileum	0.08146806	0.8517	WT-S
Duodenum vs Jejunum	0.15727534	0.5	IFNAR KO-S
Duodenum vs Ileum	0.29574362	0.2	IFNAR KO-S
Jejunum vs Ileum	0.11426463	0.7	IFNAR KO-S
Duodenum vs Jejunum	0.13241923	0.5092	F2 WT
Duodenum vs Ileum	0.21932467	0.2032	F2 WT
Jejunum vs Ileum	0.14257901	0.3164	F2 WT